Engineering Geology 242 (2018) 121–129

Contents lists available at ScienceDirect

Engineering Geology

journal homepage: www.elsevier.com/locate/enggeo

Influence of slope property variabilities on seismic sliding displacement analysis

Wenqi Du[a,*], Gang Wang[b], Duruo Huang[c]

[a] Institute of Catastrophe Risk Management, Nanyang Technological University, 50 Nanyang Avenue, 639798, Singapore
[b] Deptartment of Civil and Environmental Engineering, Hong Kong University of Science and Technology, Clear Water Bay, Hong Kong, China
[c] Department of Hydraulic Engineering, Tsinghua University, Beijing, China

ARTICLE INFO

Keywords:
Seismic slope displacement
Newmark
Fully coupled analysis
Slope properties
Parameter variability

ABSTRACT

In this study we quantitatively examined how the variabilities of slope property parameters influence the seismic slope displacement predictions based on two commonly used methods, namely the Newmark's rigid-block and the fully coupled deformable methods. A suite of 20 acceleration time-series were selected as input motions, and Monte Carlo simulations were performed to account for the influence of slope parameter variabilities. The results show that, for both Newmark's and fully coupled analyses, modeling the variability of the effective friction angle ϕ' significantly increases the geometric mean $\overline{D}$ and standard deviation $\sigma_{\ln D}$ of the resultant displacements, while modeling the variability of the other slope parameters (i.e., soil cohesion c', thickness, and water table level) results in a similar estimate of $\overline{D}$ and a slight increase of $\sigma_{\ln D}$. The other sources of uncertainty exist in fully coupled analysis are the characterizations of the average shear wave velocity V_s, and the nonlinear soil properties. Modeling the variability in nonlinear soil properties yields a reduced $\overline{D}$ estimate, and modeling the V_s variability causes a slight reduction of $\overline{D}$. Also, incorporating the variability of slope property parameters in fully coupled analysis consistently increases $\sigma_{\ln D}$, in which the variation of ϕ' plays the predominant effect. This study thoroughly quantified the influence of slope property variabilities on the computed displacements, which could help engineers in addressing the uncertainty issue in seismic slope displacement analysis.

1. Introduction

Permanent sliding displacement analysis is commonly used in assessing the seismic stability of natural slopes and earth structures. The predicted displacement, regarded as a quantitative index of seismic slope performance, has been widely used in various applications, such as the calibration of inventories of landslides triggered during previous earthquakes (e.g., Jibson et al., 2000), the identification of potential landslide zones (e.g., Jibson and Michael, 2009; Chousianitis et al., 2016; Sharifi-Mood et al., 2017), and probabilistic seismic displacement hazard analysis (e.g., Rathje and Saygili, 2008; Du and Wang, 2014; Rathje et al., 2014).

Newmark (1965) first developed a simplified method for slope displacement analysis. A rigid block is placed on an infinite plane; the block initiates to slide once the shaking acceleration exceeds a yield acceleration k_y, and it continues to move until the relative velocity becomes zero. The permanent displacement (termed as D hereafter) is calculated by integrating the episodes of an acceleration time history that exceed k_y to obtain a velocity time history, and then integrating the resultant velocity time history to obtain the cumulative displacement. The yield acceleration k_y is usually determined by solving the static limit-equilibrium equation. Many empirical models have been developed after Newmark's pioneering work (e.g., Jibson, 2007; Saygili and Rathje, 2008; Du and Wang, 2016). Since the Newmark's rigid-block model ignores the internal deformation of a sliding mass, it is most suitable for natural landslides in stiff materials (Jibson, 2011).

Flexible sliding masses generally deform internally when subjected to seismic shakings, and therefore the rigid-block assumption is not applicable. The illustration of the rigid and flexible sliding mass cases is shown in Fig. 1. For flexible/deformable sliding masses, the dynamic response of the system during seismic shaking must be accounted for appropriately. Some improved analyses including so-called decoupled and fully coupled approaches have been conducted to date (e.g., Makdisi and Seed, 1978; Rathje and Bray, 2000; Rathje and Antonakos, 2011). Specifically, the nonlinear fully coupled stick-slip deformable sliding mass model proposed by Rathje and Bray (2000) has received increasing attention recently, since it considers the deformability of the sliding mass and its periodic sliding episodes simultaneously. Bray and Travasarou (2007) reported that the fully coupled analysis could, in general, result in a reasonable estimate for the seismic performance of

* Corresponding author.
E-mail address: wqdu@ntu.edu.sg (W. Du).

https://doi.org/10.1016/j.enggeo.2018.06.003
Received 5 January 2018; Received in revised form 2 June 2018; Accepted 2 June 2018
Available online 04 June 2018

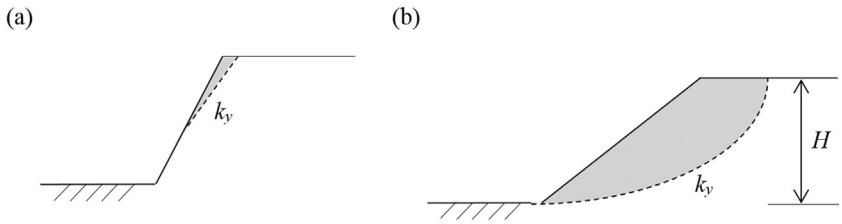

Fig. 1. Demonstration of (a) rigid, shallow sliding mass, and (b) flexible, deep sliding mass.

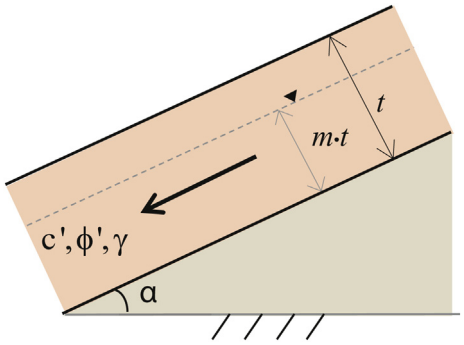

Fig. 2. Illustration of the infinite slope case with a planar failure surface.

case histories. Some predictive models have also been developed based on the fully coupled analysis (e.g., Bray and Travasarou, 2007; Du et al., 2018b).

There are several major sources of uncertainty in conducting the earthquake-induced sliding displacement analysis: (1), characterization of k_y representing the slope strength; (2) specification of ground motion intensities; and (3) characterization of a slope's initial fundamental period (T_s) and nonlinear soil properties (for flexible sliding masses only). Among these sources of uncertainty, the specification of ground motions can be well quantified by selecting a suite of input motions that properly fit a specified target response spectrum, or by conducting the fully probabilistic displacement hazard analysis (Rathje and Saygili, 2008). Yet, the influence of the other sources of uncertainty on slope displacement remains an unclear issue. Rathje and Saygili (2009) presented a probabilistic framework to quantify the uncertainty in the evaluation of sliding displacement of natural slopes. Wasowski et al. (2011) concluded that the accurate assessment of slope strength parameters plays a key role in yielding more reliable regional landslide hazard maps. Strenk and Wartman (2011) qualitatively classified the uncertainty of slope displacement predictions by considering the variation of input ground motions and slope parameters. Dreyfus et al. (2013) stated that the accurate prediction of landslide occurrence depends mostly on the shear strength assigned, and Wang and Rathje (2015) proposed a probabilistic logic-tree framework to quantify the uncertainty of slope parameters in regional landslide hazard analysis. The model uncertainty and variability in Newmark displacement analysis have also been studied recently (Du et al., 2018a). Most of the existing studies focused on the predictive uncertainty in the Newmark's rigid-block analysis, whereas such uncertainty in the fully coupled analysis for flexible sliding masses has not been well studied.

This paper aims at quantitatively studying the influence of slope property variabilities on the calculated slope displacement in the Newmark's rigid-block and fully coupled analyses. The major sources of uncertainty in the Newmark and fully coupled analyses are first identified. A suite of ground-motion recordings are then selected from the NGA-West2 database as input motions. The variations of the slope property parameters (e.g., soil strength, water table level, nonlinear soil properties) are addressed by Monte Carlo simulations, and the effect of such variations on the displacement predictions for rigid and flexible slopes is comprehensively investigated. This study quantitatively explores how the slope property variabilities influence the means and standard deviations of the computed displacements, and how to appropriately model such variabilities in practical applications.

2. Sources of uncertainty in sliding displacement analyses

2.1. Newmark's rigid-block model

As mentioned above, the Newmark's rigid-block model is most suitable for regional landslide hazard assessment. Since the dynamic deformation of a sliding mass is ignored in this model, the only source of slope property uncertainty exists in the characterization of k_y. The parameter k_y (in unit of g) can be expressed as a function of the static factor of safety (FS) and the slope's geometrical angle α:

$$k_y = (\mathrm{FS} - 1)\sin\alpha \tag{1}$$

For the infinite slope case with a planar failure surface (Fig. 2), FS can be estimated as (Jibson et al., 2000):

$$\mathrm{FS} = \frac{c'}{\gamma t \sin\alpha} + \left(1 - m\frac{\gamma_w}{\gamma}\right)\frac{\tan\phi'}{\tan\alpha} \tag{2}$$

where α denotes the slope angle of the sliding surface; c' and ϕ' are the effective cohesion and internal friction angle, respectively; γ and γ_w denote the unit weights of soil and water, respectively; t denotes the thickness normal to the failure surface; and m is the ratio of t that is below the groundwater level.

Therefore, as listed in Eqs. (1) and (2), k_y can be fully characterized based on the specification of slope parameters c', ϕ', t, m, α, and γ. For regional landslide hazard analysis, the slope angle information is usually derived from a high-resolution Digital Elevation Model (DEM) (e.g., Jibson and Michael, 2009; Wasowski and Bovenga, 2014), so the variability of α can be well constrained. The unit weight γ and shear strength parameters (c' and ϕ') are generally assigned based on the geologic unit classified, while the other parameters (t, m) are usually assigned as constant over a study area. Thus, the major sources of uncertainty in characterizing k_y are c', ϕ', t, and m. Note that the unit weight of soil γ is taken as a deterministic variable in this study, since its variability is found to be relatively small (Duncan, 2000).

2.2. Fully coupled model

In the fully coupled deformable model, the sliding mass is simplified as a generalized single-degree-of-freedom system governed by its first modal shape of vibration, and the nonlinear soil properties are usually modeled based on an equivalent-linear approach. Permanent displacement occurs when the seismic acceleration exceeds k_y. Pseudostatic slope stability analysis can be iteratively conducted using different horizontal seismic coefficients, and k_y equals the seismic coefficient that results in a FS = 1. In this study, the limit-equilibrium software *SLIDE* (Rocscience, 2010) is used for computing k_y, and the effect of the variability of slope parameters (c', ϕ', and water table level z_w) on k_y is investigated.

In addition to k_y, the characterization of the slope's fundamental period T_s is another source of uncertainty in the fully coupled analysis. T_s can be normally estimated as: $T_s = 4H/V_s$, where H and V_s are the average height and the average shear wave velocity of a sliding mass, respectively. The uncertainty of H is relatively small in applications.

Yet, many studies have reported the measurement uncertainty of V_s (Moss, 2008; Wair and DeJong, 2012). The coefficient of variation (COV) of the measured V_s uncertainty ranges from 1% to 35% depending on the different measurement techniques employed (Moss, 2008). Consequently, V_s is the major source of uncertainty in calculating T_s. The influence of the V_s profile uncertainty on other applications such as site response analysis has been studied recently (Rathje et al., 2010).

Nonlinear soil properties are commonly modeled as strain-dependent shear modulus reduction (G/G_{max} where G_{max} is the maximum shear modulus) and material damping ratio (D_r) curves. Darendeli (2001) proposed comprehensive empirical models for G/G_{max} and D_r, in which both variables are modeled as a normal distribution. The mean G/G_{max} and D_r curves are calculated based on input parameters such as plasticity index PI, overconsolidation ratio OCR, loading frequency, and mean confining pressure. The standard deviation of the normalized modulus reduction (σ_{NG}) for clays can be estimated as (Darendeli, 2001):

$$\sigma_{NG} = 0.015 + 0.164\sqrt{0.25 - (G/G_{max} - 0.5)^2} \quad (3)$$

The standard deviation of the damping ratio (σ_{D_r}) for clays is given as (Darendeli, 2001):

$$\sigma_{D_r} = 0.0067 + 0.779\sqrt{D_r} \quad (4)$$

where σ_{D_r} and D_r are in percentile form (i.e., σ_{D_r} = 3.5% for D_r as 20%). The statistical distributions of the modulus reduction and damping ratio curves for clays with PI = 30 are illustrated in Fig. 3.

In addition to Eqs. (3) and (4), the correlation between G/G_{max} and D_r (termed as ρ_{D_r}, *NG* hereafter) is another key requirement to construct the joint distribution of the simulated G/G_{max} and D_r curves. Such correlation is negative in nature.

Therefore, there are three main sources of uncertainty in the fully coupled analysis: (i), variation of slope parameters in characterizing k_y; (ii), variability of V_s in determining T_s; and (iii), variability of the G/G_{max} and D_r curves in modeling the nonlinear soil property.

3. Selection of input ground motions

A suite of well-processed ground-motion recordings are needed for sliding displacement analysis. In this study, a set of acceleration time-series are selected from the Pacific Earthquake Engineering Research Center's NGA-West2 database (Ancheta et al., 2014). Subsets of the database have been recently used for developing ground motion prediction equations for various intensity measures (e.g., Campbell and Bozorgnia, 2014; Du and Wang, 2017).

Numerous methods have been developed in selecting ground motions for dynamic time-history analysis. Some advanced methods are conducted to select ground motions that have response spectra matching a specified target distribution of response spectrum (e.g., Baker, 2011; Wang, 2011). In this effort, an earthquake scenario with moment magnitude (M_w) 7.5 on a strike-slip fault is considered. The rupture distance of a slope site considered is 5 km, and the time-averaged shear wave velocity in the upper 30 m for this site is assumed as 300 m/s. The ground motion prediction equation proposed by Campbell and Bozorgnia (2014) is adopted for predicting the target distribution of spectral accelerations.

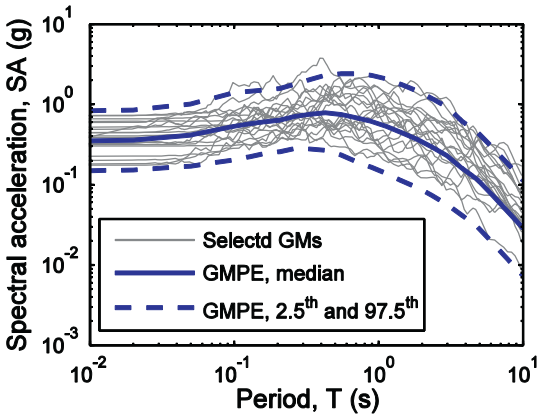

Fig. 4. Spectral distributions of selected 20 ground motions to match the target distribution under the M_w 7.5 earthquake scenario.

The ground motion selection approach proposed by Wang (2011) was used herein; 20 acceleration time-series were scaled and selected to properly match the mean and variance of the target spectrum. The response spectra of the selected ground motions are shown in Fig. 4, from which it can be seen that the selected ground motions properly represent the distribution of the target spectrum. The detailed information of these ground motions, as well as scaling factors, is summarized in Table 1. They will be used as input motions for subsequent slope displacement analysis.

4. Results of Newmark's rigid-block model

4.1. Influence of the variability of slope property parameters

The slope property parameters have a certain degree of variability that results from the inherent randomness in nature, measurement errors, sample disturbance, or course data resolution. Many studies have been conducted to characterize the variability of soil parameters (e.g., Phoon and Kulhawy, 1999a; Phoon and Kulhawy, 1999b). The typical COVs for the design soil variability of undrained shear strength and ϕ' are about 10–55% and 5–20%, respectively (Phoon and Kulhawy, 1999b). In this study, the COVs of the slope parameters (i.e., c', ϕ', t, and m) are taken as 10%, 20%, and 30%, respectively. These parameters are considered to be lognormally distributed, and the corresponding arithmetic means and COVs are listed in Table 2. Note that the

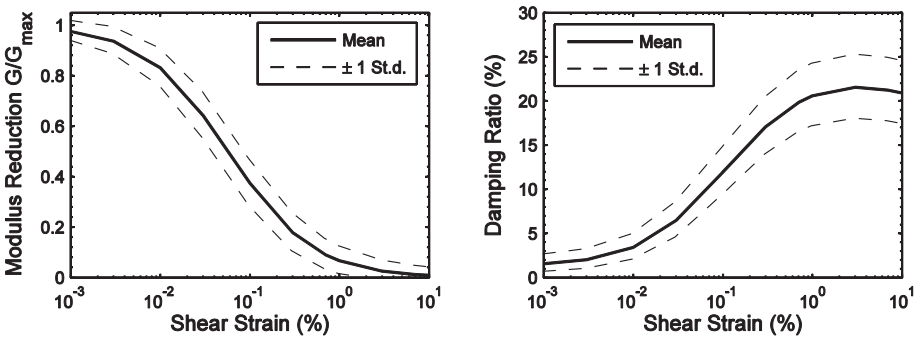

Fig. 3. Statistical distributions of the shear modulus reduction and damping ratio curves for the Darendeli (2001) model. Input parameters assigned: PI = 30, OCR = 1, loading frequency f = 1 H_z, number of cycles N = 10, and the mean confining pressure as 1 atm.

Table 1
Earthquake ground motion recordings used in this study.

RSN[a]	Earthquake event	Year	Component	Scaling factor	Scaled PGA (g)
4875	Chuetsu-oki, Japan	2007	H1	0.9	0.43
2457	Chi-Chi-03, Taiwan	1999	H2	2.3	0.43
192	Imperial Valley-06	1979	H1	2.6	0.19
1194	Chi-Chi, Taiwan	1999	H1	2.3	0.37
882	Landers	1992	H1	2.3	0.31
8606	El Mayor-Cucapah	2010	H2	0.6	0.17
175	Imperial Valley-06	1979	H2	1.5	0.17
1415	Chi-Chi, Taiwan	1999	H2	2.5	0.29
1605	Duzce, Turkey	1999	H1	2.0	0.70
2114	Denali, Alaska	2002	H1	2.2	0.70
5823	El Mayor-Cucapah	2010	H2	2.9	0.57
2458	Chi-Chi-03, Taiwan	1999	H2	3.0	0.30
1534	Chi-Chi, Taiwan	1999	H1	3.0	0.39
2114	Denali, Alaska	2002	H2	2.0	0.64
776	Loma Prieta	1989	H1	1.6	0.59
880	Landers	1992	H2	3.0	0.38
1536	Chi-Chi, Taiwan	1999	H2	2.8	0.50
1176	Kocaeli, Turkey	1999	H2	0.9	0.31
1158	Kocaeli, Turkey	1999	H1	0.7	0.22
1101	Kobe, Japan	1995	H2	1.3	0.47

[a] RSN: record sequence number in the NGA-West2 database; H1, H2: the horizontal components of ground motions classified in the NGA-West2 database; PGA: peak ground acceleration

Table 2
Statistical properties of slope parameters for Newmark's rigid-block analysis.

Parameters	Distribution	Mean	COV
c' (kPa)	Lognormal	20	0.1, 0.2, 0.3
ϕ' (°)	Lognormal	35	0.1, 0.2, 0.3
t (m)	Lognormal	4	0.1, 0.2, 0.3
m	Lognormal	0.5	0.1, 0.2, 0.3
α (°)	Deterministic	30	–
γ (kN/m^3)	Deterministic	20	–

lognormal distribution is considered herein because it guarantees that the random variables simulated are always positive.

In probability theory and statistics, for a given random variable C, COV_C is expressed as:

$$COV_C = \frac{\sigma_C}{\mu_C} \tag{5}$$

where μ_C and σ_C represent the arithmetic mean and standard deviation, respectively. If C follows a lognormal distribution, the mean and standard deviation of the natural logarithm of C are given as (Griffiths and Fenton, 2004):

$$\mu_{\ln C} = \ln \mu_C - 0.5 \ln(1 + COV_C^2) \tag{6}$$

$$\sigma_{\ln C} = \sqrt{\ln(1 + COV_C^2)} \tag{7}$$

Therefore, the arithmetic means and COVs listed in Table 2 can be used as input in Eqs. (6) and (7); Monte Carlo simulations can be further used to generate log-normally distributed slope parameters. The theoretical probability density functions of c' subjected to the COVs assigned are illustrated in Fig. 5.

For the deterministic case (the COVs of all slope parameters are 0), the calculated k_y is 0.21 g based on Eqs. (1) and (2). For probabilistic cases, several groups of k_y are calculated; for each group, the variability of one slope parameter is considered, while the best-estimate (mean) values are used for the other parameters. Boxplot, as a widely used tool in descriptive statistics, is used herein to display the distributions of k_y for the probabilistic cases. Fig. 6 shows the k_y distributions with respect to the COVs of c', ϕ', t, and m, respectively. Two observations can be made. First, the median value of k_y is generally insensitive to the change of the parameter variability, while the dispersion of k_y generally

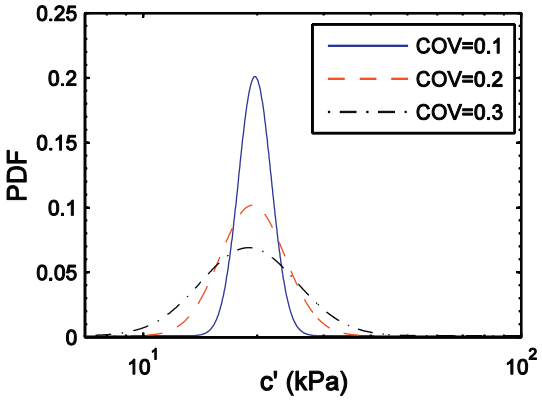

Fig. 5. Probability density functions (PDFs) of c' with different COVs.

becomes larger as COV increases. Second, it can be seen that the k_y distribution is greatly influenced by the variation of ϕ', whereas it is less influenced by the variability of the other parameters. This observation indicates that ϕ' is the major determinant for the magnitude of k_y. Note that the large COV of ϕ' considered would inevitably result in some unrealistic negative k_y values. To avoid such statically unstable cases, the few negative k_y values are assigned as 0.01 g, barely larger than zero to represent the most susceptible slopes.

The Newmark displacements were then calculated based on the ground motion suite selected and k_y groups considering the variability of slope parameters. For each group, the geometric mean $\overline{D}$ and the standard deviation of the natural logarithm of nonzero displacements ($\sigma_{\ln D}$) are calculated. Fig. 7 (a) compares the resultant $\overline{D}$ with respect to COVs for various cases. The "COV = 0" corresponds to the deterministic case (i.e., k_y = 0.21 g). The mean displacements generally keep constant as the variability of t, m, and c' increases. Yet, increasing the COV of ϕ' yields a noticeable increase in the $\overline{D}$ estimates; the means increase by about 40% and 2.8-times when the COVs of 2 and 3 are considered, respectively. This is mainly due to the large variation of k_y in such cases. As is shown in Fig. 6, the large COV of ϕ' brings in a large dispersion of k_y, including a certain portion of small k_y values (k_y < 0.1 g), which tend to result in much larger displacements. There are also a small portion of large k_y values (k_y > 0.4 g) simulated that might produce smaller displacements, but the number of these smaller values is not great enough to counteract the increase in displacements caused by the low k_y data. Therefore, $\overline{D}$ is generally larger when a larger COV of ϕ' is used.

Fig. 7 (b) displays the resultant $\sigma_{\ln D}$ with respect to COVs for various k_y groups. The calculated $\sigma_{\ln D}$ for the deterministic case is 2.6. Increasing the variability of the slope parameters generally causes an increase of $\sigma_{\ln D}$ (within the range of 0 to 25%); specifically, the variation of ϕ' has the most significant effect on the increase of $\sigma_{\ln D}$. The variation of m, in general, has a little impact on $\overline{D}$ and $\sigma_{\ln D}$ of the calculated displacements.

Compared to the deterministic case that is commonly considered in engineering applications, incorporating the variability of slope parameters in Newmark's analysis generally brings in a larger standard deviation of displacements. In particular, the statistical distribution (both $\overline{D}$ and $\sigma_{\ln D}$) of D is highly sensitive to the variation of ϕ'. Therefore, a realistic estimate of the variability of slope parameters, especially ϕ', plays an important role in accurately predicting the Newmark displacement.

4.2. Influence of correlation of c' and ϕ'

Another source of uncertainty in slope parameters is the correlation between c' and ϕ'. Many studies have reported a negative correlation between the two parameters (e.g., Cherubini, 2000). The influence of

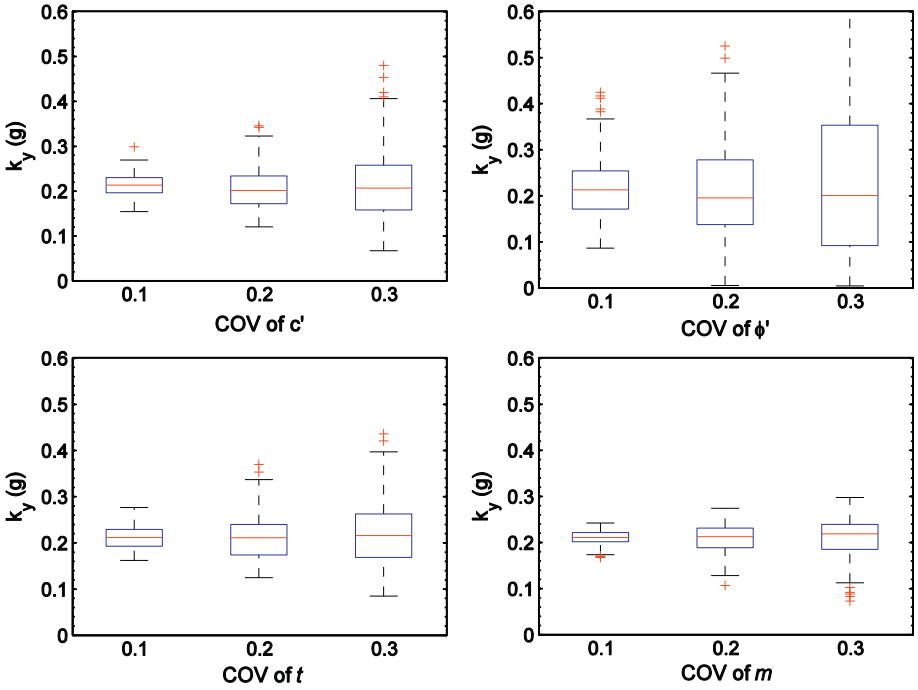

Fig. 6. Distributions of k_y based on Eqs. (1) and (2) versus the COVs of slope parameters. In these and subsequent boxplots, the central red line denotes the median of the data (50th percentile), and the edges of the box (blue lines) mark the 25th and 75th percentiles. The ends of the whiskers represent the 0.35th and 99.65th percentiles, and the red plus symbols denote outliers. (For interpretation of the references to colour in this figure legend, the reader is referred to the web version of this article.)

the c'-ϕ' correlation on Newmark displacement is therefore studied in this subsection. Three values of ρ equal to −0.5, −0.25, and 0 are considered, and the COVs of c' and ϕ' are assigned as 20% and 10%, respectively. Monte Carlo simulations were used for simulating the joint distribution of the two parameters. Fig. 8 demonstrates the distributions of the simulated c' and ϕ', respectively. It is worth noting that the mean values of the other slope parameters (e.g., t and m) listed in Table 2 are used for the calculation of k_y.

Fig. 9 shows the means and $\sigma_{\ln D}$ of Newmark displacements considering the different c'-ϕ' correlations. It is shown clearly that both $\overline{D}$ and $\sigma_{\ln D}$ increase slightly as ρ approaches 0; they increase by approximately 30% and 6% respectively when ρ changes from −0.5 to 0. A strong negative correlation means larger (smaller) c' are generally associated with smaller (larger) ϕ' (Fig. 8); these pairs of (c', ϕ') parameters tend to yield smaller dispersions of k_y and the subsequent displacement. Since c' and ϕ' are usually negatively correlated in nature, ignoring the c'-ϕ' correlation (i.e., $\rho_{c\text{-}\phi} = 0$) will result in greater estimates of the Newmark displacement.

4.3. All parameters varied

The Newmark displacements were also calculated by considering the variabilities of all slope parameters. The computed geometric means and $\sigma_{\ln D}$ are presented and compared with those obtained by considering the variability of c', ϕ', and t only in Fig. 10. Clearly, the calculated $\overline{D}$ and $\sigma_{\ln D}$ for the 'all varied' case are similar to those of modeling the variability of ϕ', and they are significantly larger than those of the other cases. These observations again confirm that the variability of ϕ' predominately influences the Newmark displacement predictions. Compared to the deterministic case, modeling low variability (COV = 0.1) of all slope parameters results in a similar $\overline{D}$ and an increase of 10% for $\sigma_{\ln D}$, while modeling high variability (COV = 0.3) of slope parameters results in a 200%-increase for $\overline{D}$, and a 30%-increase for $\sigma_{\ln D}$, respectively.

5. Results of fully coupled analysis

5.1. Influence of the variability of slope property parameters

A deep slope model with fixed geometrical parameters (Fig. 11) was implemented in *SLIDE*. The parameters assigned for this idealized slope are listed in Table 3, in which c', ϕ', and groundwater table z_w are modeled as random variables with COVs of 0.1, 0.2, and 0.3, respectively. The mean z_w location assigned is shown in Fig. 11. For the

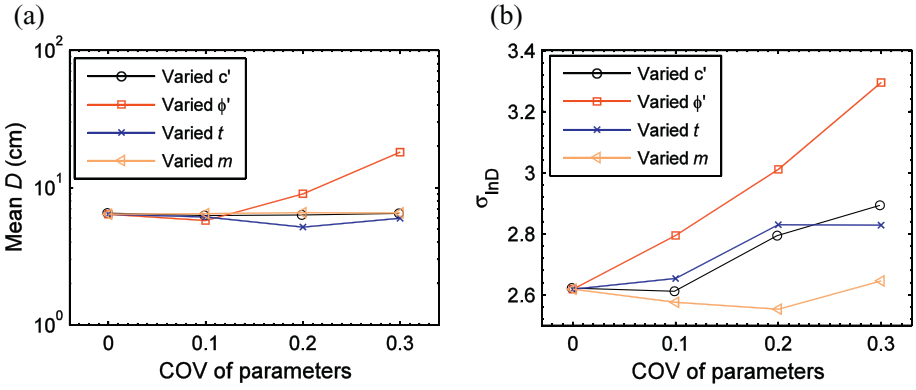

Fig. 7. Influence of the variability of slope parameters on the calculated (a) geometric mean $\overline{D}$, and (b) $\sigma_{\ln D}$ for the Newmark's rigid-block model.

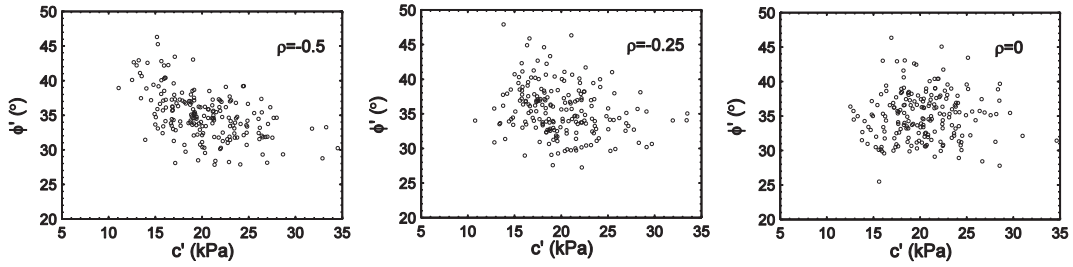

Fig. 8. Scatter plots of the simulated c' and ϕ' using ρ values of −0.5, −0.25, and 0, respectively.

deterministic case, the static FS based on the Spencer's method is 1.362, and the corresponding k_y is calculated as 0.16 g. For probabilistic cases, several groups of static FS and k_y considering the variability of slope parameters are calculated based on the probabilistic and seismic analyses implemented in *SLIDE*. The statistical distributions of k_y versus the COVs of slope parameters (i.e., c', ϕ', and z_w) are demonstrated in Fig. 12. Again, the variation of ϕ' has the greatest impact on the dispersion of k_y, while the influence of the variation of c' and z_w is much less significant.

To address the uncertainty of T_s, V_s is also modeled as a random variable with arithmetic mean as 300 m/s and COVs as 0.1, 0.2, and 0.3, respectively. Monte Carlo simulations were used for simulating sets of V_s values following the lognormal distribution. Thus, T_s can be estimated as $T_s = 4H/V_s$, and the best-estimate (mean) T_s value is 0.4 s.

The mean G/G_{max} and D_r curves shown in Fig. 3 are employed to model the nonlinear soil properties in this subsection. Fully coupled analyses were therefore performed based on the sets of k_y (considering the variations of c', ϕ', and z_w, respectively) and T_s (considering the variation of V_s). The earthquake acceleration time-series listed in Table 1 were used as input motions. Fig. 13a and b display the computed $\overline{D}$ and $\sigma_{\ln D}$ with respect to the COVs, respectively. The "COV = 0" corresponds to the deterministic case (i.e., the deep slope case with $k_y = 0.16$ g and $T_s = 0.4$ s). Similar to rigid slope cases, Fig. 13a demonstrates that increasing the variability of ϕ' brings in a significant increase in the $\overline{D}$ estimate, while the variability of c' and z_w has a little impact on $\overline{D}$. Increasing the variability of V_s causes a slight reduction in the mean estimates; such reduction reaches about 15% when the COV of V_s is 0.3. This observation is T_s-specific, which is due to the fact that peak displacement in the fully coupled analysis usually occurs at T_s in the range of 0.2–0.5 s (e.g., Bray and Travasarou, 2007), and the large dispersion of V_s simulated (associated with a large COV of V_s) brings in some T_s values out of this range, resulting in much smaller displacements. Besides, as is shown in Fig. 13b, increasing the variability of these parameters generally causes an increase on $\sigma_{\ln D}$; in particular, the change of $\sigma_{\ln D}$ is more significant with the variation of ϕ' and V_s ($\sigma_{\ln D}$ increases about 30% and 15% for COV = 0.3 of ϕ' and V_s, respectively).

5.2. Influence of correlation of c' and ϕ'

The impact of the c'-ϕ' correlation on flexible slope displacement is studied in this subsection. Three values of ρ (i.e., ρ as −0.5, −0.25, and 0, respectively) are considered, and the COVs of c' and ϕ' are assigned as 20% and 10%, respectively. The mean V_s, z_w, and the mean G/G_{max} and D_r curves are used as deterministic values. Fig. 14 displays $\overline{D}$ and $\sigma_{\ln D}$ of the resultant displacements considering the different c'-ϕ' correlations. Similar to those observed for the Newmark's analysis, decreasing the c'-ϕ' correlation causes a slight increase on the magnitude of $\overline{D}$ and $\sigma_{\ln D}$; they increase by approximately 5% and 2% respectively when ρ changes from −0.5 to 0. Thus, the influence of the c'-ϕ' correlation on the slope displacement in fully coupled analysis is little.

5.3. Influence of variability of nonlinear soil properties

The standard deviation equations listed in Eqs. (3) and (4) were used for quantifying the variability of the G/G_{max} and D_r curves, and Monte Carlo simulations were performed to account for their variability. Fig. 15 displays the means $\overline{D}$ and $\sigma_{\ln D}$ of the resultant displacements considering the variability of G/G_{max} and D_r curves, where different correlation coefficients (i.e., $\rho_{D,r}$, *NG* as −0.2, −0.5, −0.8, respectively) are considered. Compared to the deterministic case, including the variability of nonlinear soil properties yields a reduction of about 25–30% in $\overline{D}$ and an increase of about 6–15% in $\sigma_{\ln D}$. The reduction of $\overline{D}$ can be explained as follows. The randomization of G/G_{max} and D_r curves includes simulated ones with smaller G/G_{max} and higher D_r curves, which tend to experience larger strain and higher damping during seismic loading, producing much smaller displacements. Besides, increasing the$\rho_{D,r}$, *NG* correlation would bring in a slight increase of $\overline{D}$ and decrease of $\sigma_{\ln D}$, but such influence is minor.

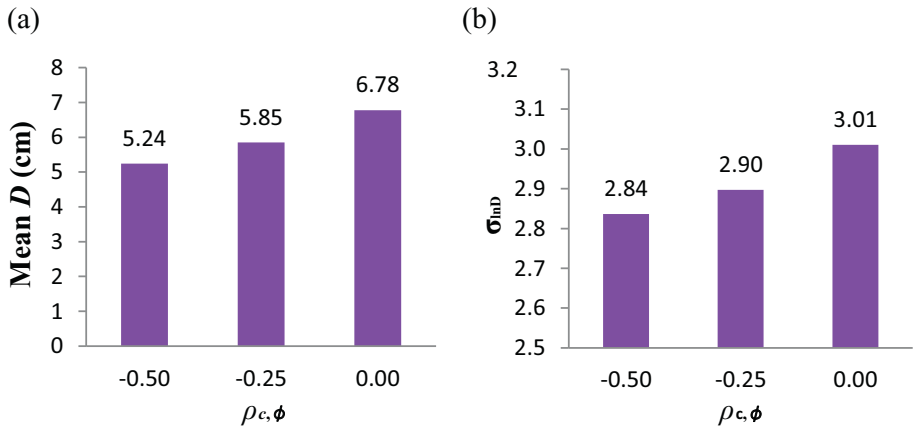

Fig. 9. Influence of the c'-ϕ' correlation on the calculated (a) geometric mean $\overline{D}$, and (b) $\sigma_{\ln D}$ based on the Newmark's rigid-block model.

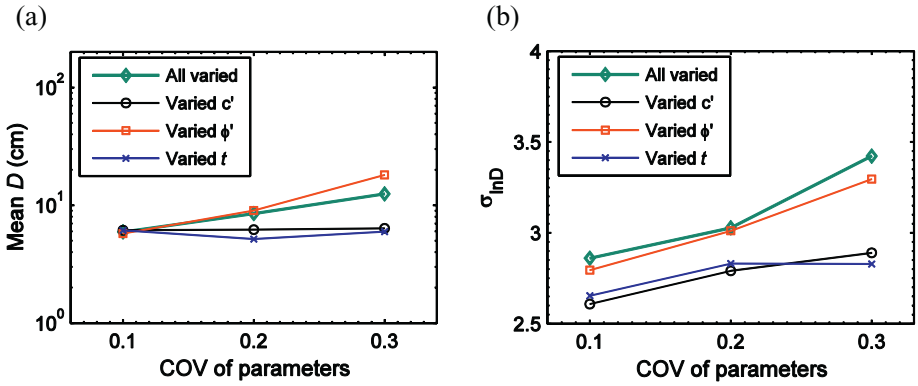

Fig. 10. Influence of different sources of uncertainty on the calculated (a) mean $\overline{D}$, and (b) $\sigma_{\ln D}$ based on the Newmark's rigid-block model.

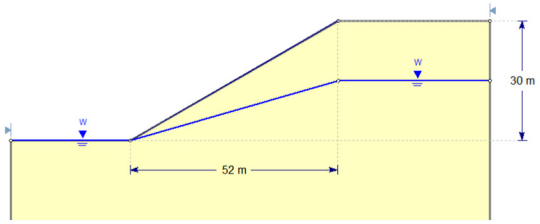

Fig. 11. Geometrically slope model used in *SLIDE* (Rocscience, 2010).

Table 3
Input parameters assigned for fully coupled analysis.

Parameters	Distribution	Mean	COV
H (m)	Deterministic	30	–
α (°)	Deterministic	30	–
γ (kN/m^3)	Deterministic	20	–
c' (kPa)	Lognormal	20	0.1, 0.2, 0.3
ϕ' (°)	Lognormal	30	0.1, 0.2, 0.3
z_w (m)	Lognormal	–	0.1, 0.2, 0.3
V_s (m/s)	Lognormal	300	0.1, 0.2, 0.3

5.4. All parameters varied

Sliding displacements can be calculated by incorporating all the sources of uncertainty in the fully coupled analysis. In this effort, the COVs of the slope property parameters (i.e., c', ϕ', z_w, and V_s) are assigned as 0.2 ($\rho_{c',\phi'} = -0.5$). The correlation of $\rho_{D,}$ *NG* as -0.5 is used for the simulation of modulus reduction and damping ratio curves. Fig. 16 displays the resultant $\overline{D}$ and $\sigma_{\ln D}$ for (A) the deterministic case; considering the variability of (B) k_y (variations of c', ϕ', and z_w); (C) T_s (variation of V_s); (D) G/G_{max} and D_r curves; and (E) all of these parameters. Compared to the deterministic case, considering the variability of k_y brings in a 40%-increase in the $\overline{D}$ estimates, while incorporating the variability of G/G_{max} and D_r curves yields a noticeable reduction in $\overline{D}$. The calculated $\sigma_{\ln D}$ for cases B-E are, as expected, larger than that of case A. The fully varied case (case E) results in a slight decrease of $\overline{D}$ (about 15% smaller than case A) and an increase of $\sigma_{\ln D}$ (about 10% greater than case A).

6. Discussions

Modeling the variability of slope property parameters is an important issue in accurately predicting the earthquake-induced slope displacement. Previous studies have mainly focused on quantifying the variabilities in ground motion and displacement predictions for probabilistic displacement hazard analysis (e.g., Rathje and Saygili, 2008; Du and Wang, 2014), while the variabilities in characterizing k_y, T_s, and nonlinear soil properties have not been well addressed. For Newmark's rigid-block analysis, the results show that modeling the variability of ϕ' has the greatest influence on $\overline{D}$ and $\sigma_{\ln D}$ of the computed displacements, while the variability of c' and t has the secondary influence. Specifically, when performing the regional landslide hazard analysis, ignoring the variability of ϕ' in the Newmark displacement analysis may significantly underpredict the landslide hazard. Therefore, a reliable characterization of the slope parameter variability is required in the Newmark's approach, and the logic-tree approach for regional mapping of landslide hazards (Wang and Rathje, 2015) is recommended.

For the fully coupled analysis, the results indicate that modeling the variability of k_y greatly increases the $\overline{D}$ estimates, while modeling the variability of the nonlinear soil properties decreases $\overline{D}$. On the other hand, considering the variability of these parameters generally results in an increase of $\sigma_{\ln D}$. Hence, these parameter variabilities need to be carefully quantified in the fully coupled analysis, to obtain the best estimate of slope displacement.

The observations above for the fully coupled analysis are specific to the slope period and the earthquake scenario considered, because both T_s and shaking intensities can greatly influence the degree of nonlinearity induced. The influence of V_s variability on slope displacement is therefore T_s-specific, and more research activities are required in future.

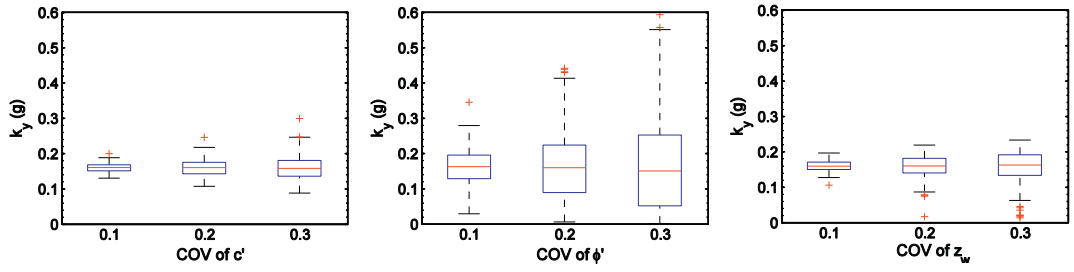

Fig. 12. Distributions of k_y for the slope case implemented in *SLIDE* versus the COVs of slope parameters c', ϕ', and z_w.

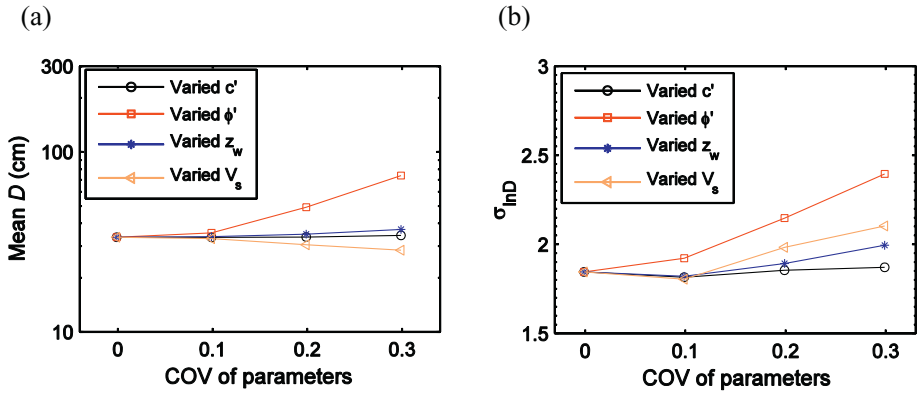

Fig. 13. Influence of the variability of slope parameters on the calculated (a) mean $\overline{D}$, and (b) $\sigma_{\ln D}$ based on the fully coupled model.

It is worth noting that although the variability of the slope angle α is not considered in this study, such variability is no doubt an important factor in charactering k_y, and further influencing the sliding displacement. The use of a high-resolution DEM to extract accurate information about slope angles is highly recommended for regional seismic landslide analysis.

In this study, the slope parameters (e.g., c', ϕ', t) are assumed to follow a lognormal distribution. Although lognormal distribution is one of the commonly used choices to characterize soil parameters in geotechnical engineering, it might be not applicable to some cases. Further research effort is therefore required regarding the appropriate distribution of these slope parameters.

7. Conclusions

This paper quantitatively studied the influence of slope property variabilities on earthquake-induced sliding displacements based on two commonly used methods, namely the Newmark's rigid-block and the fully coupled equivalent-linear analyses. An input motion suite with 20 acceleration time-series was selected and scaled to fit the target response spectrum under an M_w 7.5 earthquake scenario. A series of Monte Carlo simulations were performed to characterize the slope property variabilities, and the influence of such variabilities on the calculated displacements for rigid and flexible slopes was evaluated.

The characterization of k_y is the only source of slope property uncertainty in the Newmark displacement analysis. Results of these analyses demonstrate that incorporating the variability of ϕ' results in noticeably larger estimates of the geometric mean $\overline{D}$ and the standard deviation $\sigma_{\ln D}$; they increase by 40% and 16% respectively when the COV of ϕ' is considered as 0.2. Considering the variability of the other slope parameters (i.e., c', t, and m) yields similar estimates of $\overline{D}$, and a slight increase ($< 10\%$) of $\sigma_{\ln D}$. In addition, it was found that increasing the negative c'-ϕ' correlation slightly decreases the estimates of $\overline{D}$ and $\sigma_{\ln D}$. Therefore, the variability of ϕ' has the largest influence on the calculated displacement. When performing the regional landslide hazard analysis, the variability of slope parameters, especially ϕ', needs to be appropriately incorporated in conducting the Newmark analysis.

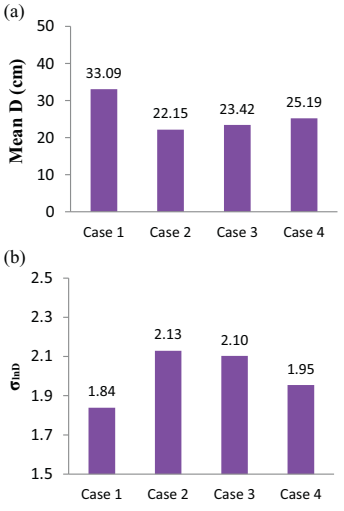

Case	Description
1	Deterministic
2	Varied soil nonlinearity with $\rho_{Dr,NG}$= -0.2
3	Varied soil nonlinearity with $\rho_{Dr,NG}$= -0.5
4	Varied soil nonlinearity with $\rho_{Dr,NG}$= -0.8

Fig. 15. Influence of the variability of nonlinear soil properties on the calculated (a) $\overline{D}$, and (b) $\sigma_{\ln D}$ based on the fully coupled model.

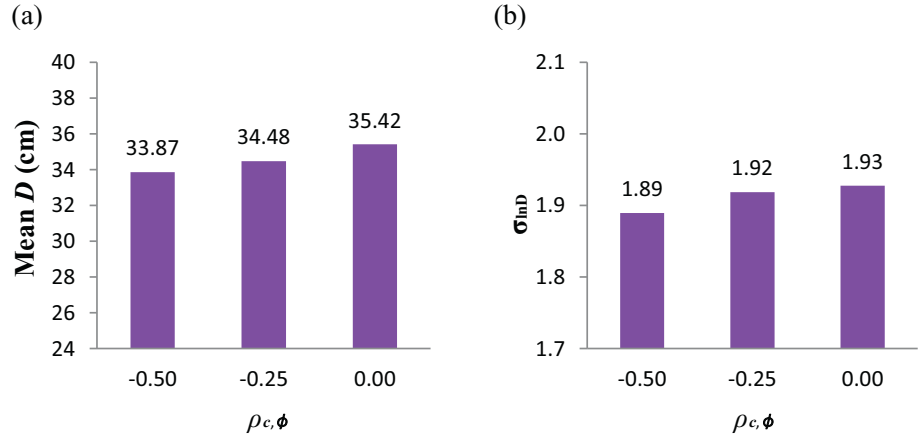

Fig. 14. Influence of the c'-ϕ' correlation on the calculated (a) geometric mean $\overline{D}$, and (b) $\sigma_{\ln D}$ based on the fully coupled model.

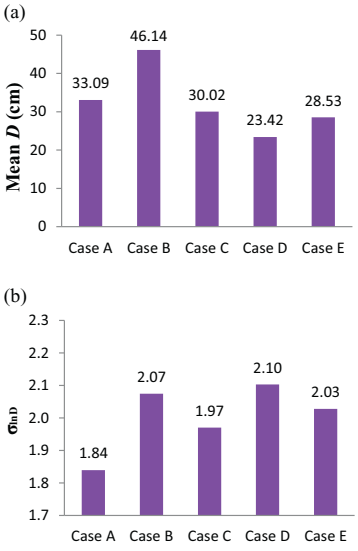

Case	Description
A	Deterministic
B	Varied k_y
C	Varied T_s
D	Varied G/G_{max} and D_r
E	All Varied

Fig. 16. Influence of different sources of uncertainty on the calculated (a) geometric mean $\overline{D}$, and (b) $\sigma_{\ln D}$ based on the fully coupled model.

The main sources of uncertainty considered in the fully coupled analysis are the characterizations of k_y (variations of c', ϕ' and z_w,), T_s (variation of V_s), and the specification of nonlinear soil properties. The results imply that the effective friction angle ϕ' is the controlling parameter for the variation of k_y. Modeling the variability of ϕ' and the nonlinear soil properties brings in a noticeable increase (40% larger if the COV of ϕ' is 0.2) and decrease (about 25–30% smaller) of the $\overline{D}$ estimates, respectively. For the deformable slope case considered (T_s = 0.4 s), modeling the variability of V_s causes a slight reduction of $\overline{D}$. Besides, modeling the variability of these parameters consistently increases $\sigma_{\ln D}$ of the calculated displacements, with $\sigma_{\ln D}$ increasing as large as 30% in some cases. Specifically, incorporating the variability of ϕ', V_s, and the nonlinear soil properties plays the major effect on the increase of $\sigma_{\ln D}$. In addition, it was found that the c'-ϕ' and G/G_{max}-D_r correlations generally have a minor effect on the resultant displacement.

The findings described above address the uncertainty issue in conducting slope displacement analyses. Based on the results and suggestions, engineers can make their judgment to properly account for the variability of slope parameters in engineering applications, in order to achieve a more accurate estimate of the seismic slope displacement.

Acknowledgments

This work was supported by Hong Kong Research Grants Council through General Research Fund 16213615. The authors greatly thank the Journal Editor and two anonymous reviewers for their helpful comments to improve this manuscript.

References

Ancheta, T.D., Darragh, R.B., Stewart, J.P., Seyhan, E., Silva, W.J., Chiou, B.S.J., et al., Donahue, J.L., 2014. NGA-West2 database. Earthquake Spectra 30 (3), 989–1005.
Baker, J.W., 2011. Conditional mean spectrum: tool for ground-motion selection. J. Struct. Eng. 137 (3), 322–331.
Bray, J.D., Travasarou, T., 2007. Simplified procedure for estimating earthquake-induced deviatoric slope displacements. J. Geotech. Geoenviron. 133, 381–392.
Campbell, K.W., Bozorgnia, Y., 2014. NGA-West2 ground motion model for the average horizontal components of PGA, PGV, and 5% damped linear acceleration response spectra. Earthquake Spectra 30 (3), 1087–1115.
Cherubini, C., 2000. Reliability evaluation of shallow foundation bearing capacity on c' φ' soils. Can. Geotech. J. 37 (1), 264–269.
Chousianitis, K., Del Gaudio, V., Sabatakakis, N., Kavoura, K., Drakatos, G., Bathrellos, G.D., Skilodimou, H.D., 2016. Assessment of earthquake-induced landslide hazard in Greece: from arias intensity to spatial distribution of slope resistance demand. Bull. Seismol. Soc. Am. 106 (1), 174–188.
Darendeli, M.B., 2001. Development of a New Family of Normalized Modulus Reduction and Material Damping Curves. University of Texas at Austin, Austin, Texas (Ph.D. thesis).
Dreyfus, D., Rathje, E.M., Jibson, R.W., 2013. The influence of different simplified sliding-block models and input parameters on regional predictions of seismic landslides triggered by the Northridge earthquake. Eng. Geol. 163, 41–54.
Du, W., Wang, G., 2014. Fully probabilistic seismic displacement analysis of spatially distributed slopes using spatially correlated vector intensity measures. Earthq. Eng. Struct. Dyn. 43 (5), 661–679.
Du, W., Wang, G., 2016. A one-step Newmark displacement model for probabilistic seismic slope displacement hazard analysis. Eng. Geol. 205, 12–23.
Du, W., Wang, G., 2017. Prediction equations for ground-motion significant durations using the NGA-West2 database. Bull. Seismol. Soc. Am. 107 (1), 319–333.
Du, W., Huang, D., Wang, G., 2018a. Quantification of model uncertainty and variability in Newmark displacement analysis. Soil Dyn. Earthq. Eng. 109, 286–298.
Du, W., Wang, G., Huang, D., 2018b. Evaluation of seismic slope displacements based on fully coupled sliding mass analysis and NGA-West2 database. J. Geotech. Geoenviron. Eng. Published Online. http://dx.doi.org/10.1061/(ASCE)GT.1943-5606.0001923.
Duncan, J.M., 2000. Factors of safety and reliability in geotechnical engineering. J. Geotech. Geoenviron. 126 (4), 307–316.
Griffiths, D.V., Fenton, G.A., 2004. Probabilistic slope stability analysis by finite elements. J. Geotech. Geoenviron. 130 (5), 507–518.
Jibson, R.W., 2007. Regression models for estimating coseismic landslide displacement. Eng. Geol. 91, 209–218.
Jibson, R.W., 2011. Methods for assessing the stability of slopes during earthquakes-a retrospective. Eng. Geol. 122 (1), 43–50.
Jibson, R.W., Michael, J.A., 2009. Maps showing seismic landslide hazards in anchorage, Alaska. In: U.S. Geological Survey Scientific Investigations Map. vol. 3077 (11 pp.).
Jibson, R.W., Harp, E.L., Michael, J.A., 2000. A method for producing digital probabilistic seismic landslide hazard maps. Eng. Geol. 58 (3), 271–289.
Makdisi, F.I., Seed, H.B., 1978. Simplified procedure for estimating dam and embankment earthquake-induced deformations. J. Geotech. Eng. Div. 104 (7), 849–867.
Moss, R.E.S., 2008. Quantifying measurement uncertainty of thirty-meter shear-wave velocity. Bull. Seismol. Soc. Am. 98 (3), 1399–1411.
Newmark, N.M., 1965. Effects of earthquakes on dams and embankments. Géotechnique 15 (2), 139–160.
Phoon, K.K., Kulhawy, F.H., 1999a. Characterization of geotechnical variability. Can. Geotech. J. 36, 612–624.
Phoon, K.K., Kulhawy, F.H., 1999b. Evaluation of geotechnical property variability. Can. Geotech. J. 36 (4), 625–639.
Rathje, E.M., Antonakos, G., 2011. A unified model for predicting earthquake-induced sliding displacements of rigid and flexible slopes. Eng. Geol. 122 (1), 51–60.
Rathje, E.M., Bray, J.D., 2000. Nonlinear coupled seismic sliding analysis of earth structures. J. Geotech. Geoenviron. 126 (11), 1002–1014.
Rathje, E.M., Saygili, G., 2008. Probabilistic seismic hazard analysis for the sliding displacement of slopes: scalar and vector approaches. J. Geotech. Geoenviron. 134 (6), 804–814.
Rathje, E.M., Saygili, G., 2009. Probabilistic assessment of earthquake-induced sliding displacements of natural slopes. Bull. N. Z. Soc. Earthq. Eng. 42 (1), 18–27.
Rathje, E.M., Kottke, A.R., Trent, W.L., 2010. Influence of input motion and site property variabilities on seismic site response analysis. J. Geotech. Geoenviron. 136 (4), 607–619.
Rathje, E.M., Wang, Y., Stafford, P.J., Antonakos, G., Saygili, G., 2014. Probabilistic assessment of the seismic performance of earth slopes. Bull. Earthq. Eng. 12 (3), 1071–1090.
Rocscience, 2010. SLIDE-2D Limit Equilibrium Slope Stability Analysis, Version 6.0. Rocscience, Inc, Toronto.
Saygili, G., Rathje, E.M., 2008. Empirical predictive models for earthquake-induced sliding displacements of slopes. J. Geotech. Geoenviron. 134 (6), 790–803.
Sharifi-Mood, M., Olsen, M.J., Gillins, D.T., Mahalingam, R., 2017. Performance-based, seismically-induced landslide hazard mapping of Western Oregon. In: Soil Dynamics and Earthquake Engineering103, pp. 38–54.
Strenk, P.M., Wartman, J., 2011. Uncertainty in seismic slope deformation model predictions. Eng. Geol. 122 (1), 61–72.
Wair, B.R., DeJong, J.T., 2012. Guidelines for estimation of shear wave velocity profiles. Pacific earthquake engineering research center. Report 08 (2012).
Wang, G., 2011. A ground motion selection and modification method capturing response spectrum characteristics and variability of scenario earthquakes. Soil Dyn. Earthq. Eng. 31 (4), 611–625.
Wang, Y., Rathje, E.M., 2015. Probabilistic seismic landslide hazard maps including epistemic uncertainty. Eng. Geol. 196, 313–324.
Wasowski, J., Bovenga, F., 2014. Investigating landslides and unstable slopes with satellite multi temporal interferometry: current issues and future perspectives. Eng. Geol. 174, 103–138.
Wasowski, J., Keefer, D.K., Lee, C.T., 2011. Toward the next generation of research on earthquake-induced landslides: current issues and future challenges. Eng. Geol. 122 (1), 1–8.